Low affinity uniporter carrier proteins can increase net substrate uptake rate by reducing efflux

Bosdriesz, Evert; Wortel, Meike T.; Haanstra, Jurgen R.; Wagner, Marijke J.; De La Torre, Pilar; Teusink, Bas

DOI
10.1038/s41598-018-23528-7

Publication date
2018

Document Version
Final published version

Published in
Scientific Reports

SCIENTIFIC REPORTS

OPEN

Low affinity uniporter carrier proteins can increase net substrate uptake rate by reducing efflux

Received: 10 November 2017
Accepted: 9 March 2018
Published online: 03 April 2018

Evert Bosdriesz[1,3], Meike T. Wortel[1,4], Jurgen R. Haanstra[1], Marijke J. Wagner[1], Pilar de la Torre Cortés[2] & Bas Teusink[1]

Many organisms have several similar transporters with different affinities for the same substrate. Typically, high-affinity transporters are expressed when substrate is scarce and low-affinity ones when it is abundant. The benefit of using low instead of high-affinity transporters remains unclear, especially when additional nutrient sensors are present. Here, we investigate two hypotheses. It was previously hypothesized that there is a trade-off between the affinity and the catalytic efficiency of transporters, and we find some but no definitive support for it. Additionally, we propose that for uptake by facilitated diffusion, at saturating substrate concentrations, lowering the affinity enhances the net uptake rate by reducing substrate efflux. As a consequence, there exists an optimal, external-substrate-concentration dependent transporter affinity. A computational model of *Saccharomyces cerevisiae* glycolysis shows that using the low affinity HXT3 transporter instead of the high affinity HXT6 enhances the steady-state flux by 36%. We tried to test this hypothesis with yeast strains expressing a single glucose transporter modified to have either a high or a low affinity. However, due to the intimate link between glucose perception and metabolism, direct experimental proof for this hypothesis remained inconclusive. Still, our theoretical results provide a novel reason for the presence of low-affinity transport systems.

Cells need to acquire all their nutrients and energy sources from the environment. Since hardly any of these can diffuse freely through the membrane, nutrient uptake requires transporter proteins. Often, a cell has several different transporters for the same nutrient. A recurring phenomemon is that these different transporters have different affinities. For example, the yeast *Saccharomyces cerevisiae* has 17 different glucose transporters[1], with Michealis-Menten constants (K_M, the substrate concentration at which the half-maximal uptake rate is attained in the absence of product inhibition) ranging from $K_M \approx 1$ mM for the highest to $K_M \approx 100$ mM for the lowest affinity transporters. Other examples of nutrient transport by both high and low affinity transporters are glucose uptake in human cells[2] and in *Lactococcus lactis*[3], phosphate and zinc uptake in yeast[4], and lactate transport in mammalian cells[5,6]. The *Arabidopsis* nitrate transporter CHL1 was shown to be able to switch between a high and low affinity mode of action through phosphorylation of the protein[7]. Typically, the high affinity transporters are expressed under conditions of low substrate availability and the low affinity transporters when substrate is plentiful. While the benefit of employing a high affinity transporter under substrate scarcity is evident, the reason for switching to low affinity transporters when substrate is more abundant remains unclear. Why is a high affinity transporter not always preferable over a low affinity one?

Previously, several hypotheses have been suggested to explain the benefit of using low affinity carriers. One hypothesis states that these increase the ability of cells to sense extracellular substrates. Levy *et al*. convincingly show that low affinity carriers for phosphate and zinc allow the cell to sense depletion of phosphate and zinc early, and consequently, the cells can adapt their physiology to a phosphate or zinc-poor environment[4]. However, for substrates with a higher import rate, such as glucose, there might be a stronger selection pressure on efficiency

[1]Systems Bioinformatics, Amsterdam Institute for Molecules, Medicines and Systems (AIMMS), VU University, Amsterdam, De Boelelaan 1108, 1081HZ, The Netherlands. [2]Department of Biotechnology, Delft University of Technology, Delft, The Netherlands. [3]Present address: Division of Molecular Carcinogenesis, The Oncode Institute, The Netherlands Cancer Institute, Amsterdam, The Netherlands. [4]Present address: Centre for Ecological and Evolutionary Synthesis (CEES), The Department of Biosciences, University of Oslo, Blindernveien 31, 0371, Oslo, Norway. Evert Bosdriesz and Meike T. Wortel contributed equally to this work. Correspondence and requests for materials should be addressed to B.T. (email: b.teusink@vu.nl)

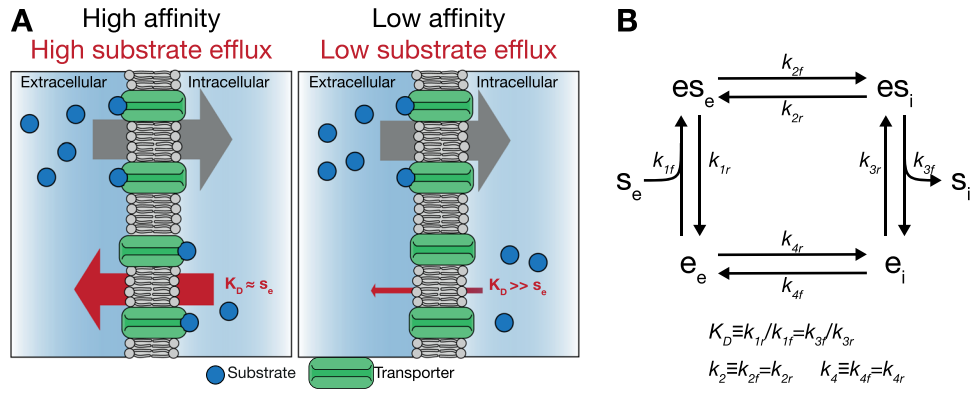

Figure 1. Lower affinity can enhance uptake by reducing substrate efflux. (**A**) Illustration of the reduced-efflux hypothesis. Left panel: A high affinity of the transporter will cause both the inward facing and the outward facing binding sites of the transporter to be saturated with substrate. As a result, the efflux rate will be nearly as high as the influx rate, and the net uptake rate is very low. Right panel: Reducing the affinity of the transporter reduces the saturation of the transporter at the intracellular side. Provided the extracellular substrate concentration is high enough, the transporter will still be saturated at the extracellular side. The efflux will be reduced and the net uptake rate increases. (**B**) Model of nutrient transport by facilitated diffusion underlying Equation 1. The transporter switches between conformations with an inward-facing (e_i) and outward-facing (e_e) substrate binding site. When this conformation change takes places with an occupied substrate binding site (es_e or es_i), this results in translocation of the substrate over the membrane. All steps are reversible and the state transitions rates are given by mass action kinetics. Throughout the main text, we make the assumption that binding is much faster than transport and that the carrier is symmetric. The former assumption allows us to use the quasi steady-state assumption for substrate to transporter binding, *i.e.* e_x and es_x are in equilibrium, with dissociation constant $k_D \equiv k_{1r}/k_{1f} = k_{3f}/k_{3r}$. The latter assumption implies $k_{2f} = k_{2r} \equiv k_2$ and $k_{4f} = k_{4r} \equiv k_4$.

of uptake than on accurate sensing. Moreover, or perhaps consequently, separate extracellular substrate sensors have been described (for example in *S. cerevisiae*[1]), and glucose sensing and uptake in *S. cerevisiae* are known to be uncoupled[8].

A second hypothesis is related to transporter efficiency, and states that there is a trade-off between the affinity and maximal uptake rate per unit-transporter (k_{cat}) of a transporter (suggested by Gudelj *et al.*[9] based on data by Elbing *et al.*[10]). The cell membrane is a crowded place, and valuable space taken up by a particular membrane protein cannot be used by another one[11]. This implies that, besides the expenditure of energy and precursor metabolites, expression of membrane transporter proteins entails an additional cost, and there is a strong selective pressure to maximize the uptake flux per unit transporter expressed in the membrane. Under high substrate availability, it is beneficial to switch to low-affinity, high-k_{cat} transporters. While there is some theoretical support for a rate-affinity trade-off for particular reaction schemes[12,13], this depends on untestable assumptions about the free energy profile and it does not apply to typical reaction schemes of membrane transport processes, such as facilitated diffusion. We will study the theoretical and experimental basis of this trade-off for transport by means of facilitated diffusion.

These hypotheses do not convincingly explain the presence of many distinct carriers in, for example, *S. cerevisiae*. In this paper, we present a new hypothesis based on the reversibility of the transport process. We focus in particular on facilitated diffusion, an often occurring mechanism of which glucose uptake in yeast and human cells are examples. We suggest that an increased affinity not only increases the rate of the substrate influx into the cell, but also that of substrate efflux out of the cell. Due to the nature of a substrate carrier, the impact of the outward transport remains significant even at saturating extracellular concentrations[14]. Therefore, we cannot neglect the outward transport solely because extracellular concentrations are much higher than intracellular concentrations. We argue that the main difference between high- and low-affinity facilitated-diffusion transporters is that for the high-affinity transporters often both sides are saturated with substrate, while for the low-affinity transporter only the extracellular side is. At the same (high) extracellular substrate concentration the low-affinity transporter would therefore have a higher import activity. This reasoning is graphically depicted in Fig. 1A. With this hypothesis we challenge the intuitive assumption that a higher affinity always leads to a higher net uptake rate.

Results

Mathematical model of facilitated diffusion kinetics. Transport of substrate s over a membrane by means of facilitated diffusion can generally be described by a four-step process (depicted in Fig. 1B). These steps are: (i) extracellular substrate s_e to carrier binding, (ii) transport of s over the membrane, (iii) release of s in the cytosol and (iv) return of the substrate-binding site to the periplasm-facing position. Note that step (iv) is the only step that distinguishes this scheme from reversible Michaelis-Menten kinetics. We will later discuss the significance of this distinction.

Thermodynamics dictate that all individual steps are reversible. Moreover, there is no energy input in this transport cycle, so the equilibrium constant $K_{eq} = 1$. For convenience, we will make two biologically-motivated

assumptions that considerably simplify the rate equation in terms of the first order rate constants. However, relaxing these assumptions does not qualitatively alter our conclusions (cf. Supplementary Information). The assumptions are: (a) binding and unbinding of the substrate to the transporter is much faster than transport of the substrate over the membrane, i.e., binding is assumed to be in quasi steady state, and (b) the transport process is symmetrical. This implies two things, the intra- and extracellular substrate-transporter-dissociation constants are equal and the forward and reverse rate constants of steps (ii) and (iv) are equal, i.e., $k_{2f} = k_{2r} \equiv k_2$ and $k_{4f} = k_{4r} \equiv k_4$. The latter assumption is sensible because the "substrate" and the "product" of the transportation step are chemically identical. Therefore, there is no a priori reason why e.g., extracellularly the substrate should bind tighter to the carrier than intracellularly. The consequence of this assumption is that the K_M of substrate influx and substrate efflux are equal. For e.g., hexose transport in *S. cerevisiae* this is indeed the case for all 7 Hxt carriers that were characterized by Maier *et al.*[15] (also see[10]). The rate equation takes the form

$$v = e_t \cdot \frac{\frac{k_{cat}}{K_M}(s_e - s_i)}{1 + \frac{s_e}{K_M} + \frac{s_i}{K_M} + \alpha\frac{s_e \cdot s_i}{K_M^2}}, \tag{1}$$

with

$$k_{cat} = \frac{k_2 k_4}{k_2 + k_4} \tag{2a}$$

$$K_M = 2K_D\frac{k_4}{k_2 + k_4} \tag{2b}$$

$$\alpha = 4\frac{k_2 k_4}{(k_2 + k_4)^2} \tag{2c}$$

Where $K_D \equiv \frac{k_{1r}}{k_{1f}} = \frac{k_{3f}}{k_{3r}}$ is the dissociation constant of transporter-substrate binding.

The trade-off hypothesis: The theoretical basis of the trade-off between rate and affinity. A comparison of Equations (2a) and (2b) immediately shows both the strength and the weakness of the hypothesis that there is a trade-off between the k_{cat} and the affinity of a transporter. Since both $\frac{dk_{cat}}{dk_4}$ and $\frac{dK_M}{dk_4}$ are always positive, any mutation that increases k_4 enhances the k_{cat} but reduces the affinity. In that sense, there might be a rate-affinity trade-off. However, any mutation that decreases the K_D enhances the transporters affinity without affecting the k_{cat}, and since $\frac{dk_{cat}}{dk_2}$ is always positive but $\frac{dK_M}{dk_2}$ is always negative, an increase in k_2 enhances both the affinity and the k_{cat}. This means that only if k_2 and K_D are constrained by biophysical limitations, there is a real trade-off between rate and affinity. Whether or not this is the case is generally difficult to establish. An additional confounding factor is the α-term, which describes the asymmetry between an occupied and an unoccupied carrier and which is affected by any mutations affecting k_2 and k_4. While α does not affect the k_{cat} and K_M, it does affect the uptake rate. The higher it is (i.e., the larger the asymmetry), the lower the uptake rate.

When the assumptions of fast substrate to transporter binding and symmetry are dropped, an analytic evaluation of this trade-off becomes infeasible. The macroscopic kinetic parameters depend in a complicated way on the first order rate constants, and the latter are interdependent. A parameter sampling approach indicates that also in this case there are some rate-constants for which a trade-off can be found, while for others this is not the case (Supplementary Figure S1). We refer to the Supplementary Information for a more detailed discussion.

The reduced efflux hypothesis: A lowered affinity can enhance the net uptake rate by reducing substrate efflux. When discussing the transporter's k_{cat} and affinity in terms of a trade-off, one makes the implicit assumption that for flux maximization a high affinity is, all else being equal, always better than a low affinity. While this might sound like an obvious statement it is, in fact, not true; decreasing the affinity of the transporter without affecting the k_{cat} can actually enhance the net uptake rate.

To see why, consider a high affinity transporter fully saturated with extracellular substrate. Now, suppose that the intracellular substrate concentration is much lower than the extracellular, but still well above the K_M of the transporter, i.e. $s_e \gg s_i \gg K_M$. In this situation, each time the transporter moves its binding site over the membrane a substrate molecule will be transported, regardless of whether it moves from the outside to the inside, or the other way around. Hence, despite a considerable concentration gradient, the influx and efflux rates will be nearly equal, and the net uptake rate will be close to zero. In other words, the transporter is severely inhibited by its product. In contrast, consider the same situation, but now with a low-affinity transporter, which has a K_M above the intracellular glucose concentration, but still well below that of extracellular glucose, $s_e \gg K_M > s_i$. In this case, the transporter will operate close to its maximal possible uptake rate (V_{max}), because it's forward rate is saturated, but the efflux rate is low. This reasoning is graphically depicted in Fig. 1A.

The argument above implies that there is a condition-dependent optimal affinity, K_M^{opt}, for the transporter, which maximizes the net uptake rate as a function of intracellular and extracellular substrate concentration. This is given by (cf. Supplementary Information):

$$K_M^{opt} = \sqrt{\alpha \cdot s_e \cdot s_i} \tag{3}$$

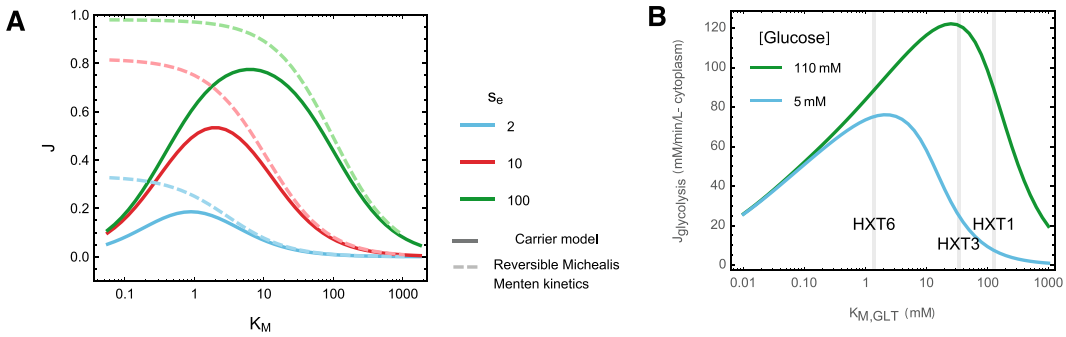

Figure 2. High affinities can reduce the net uptake rate in facilitated diffusion models. (**A**) Steady-state uptake rate (J) as a function of the Michaelis-Menten contant (K_M, the substrate concentration at which the half-maximal uptake rate is attained in the absence of product inhibition) of a facilitated diffusion model (solid lines) and with reversible Michaelis Menten kinetics (dashed lines), for different external substrate concentrations s_e and a constant internal substrate concentration $s_i = 1$. In a facilitated diffusion model very high affinities reduce the steady state flux, whereas for reversible Michaelis-Menten kinetics J monotonically decreases with K_M. The K_M was varied by varying the substrate-transporter dissociation-constants K_D, which for both rate equations affects the K_M but not the maximal uptake rate per transporter (k_{cat}). We used $k_2 = 1$ and $k_4 = 8$ and a total transporter concentration $e_t = 1$. (**B**) Steady-state flux $J_{glycolysis}$, as a function of the Michaelis-Menten constant of the glucose transporter $K_{M,GLT}$, of a kinetic model of *S. cerevisiae* glycolysis. At an extracellular glucose concentration of 110 mM (green line) the low affinity HXT3 transporter ($K_M = 34$ mM) is roughly optimal, with $J_{glycolysis} = 121$ mM/min/L-cytosol, whereas the high affinity HXT6 transporter ($K_M = 1.4$ mM) attains $J_{glycolysis} = 88.8$ mM/min/Lcytosol. At low glucose concentrations (blue line) the high affinity transporter performs better.

Figure 2A (solids lines) visualizes this relation between the K_M, the steady-state uptake rate J, and the external substrate concentration s_e. Below a certain value, reducing the K_M reduces J, and as K_M approaches 0, so does J. At which K_M-value the maximal J is attained depends on s_e. This is in stark contrast to reversible Michaelis-Menten kinetics, where an increased affinity always increases the uptake rate (Fig. 2A, dashed lines). As noted previously, the fundamental difference between these two models is the step between intracellular substrate release and relocation of the binding site to the extracellular side of the membrane. (The reversible the Michaelis-Menten rate equation is identical to Equation 1 except it lacks the $\alpha \cdot s_e \cdot s_i/K_M^2$-term). In the carrier model, intra- and extracellular substrates are not directly competing for the same binding sites, and the substrate efflux rate is in effect insensitive to the extracellular substrate concentration. This explains the qualitatively different behavior of the two kinetic schemes. The result that there is an optimal affinity of the transporter also holds for the non-symmetric carrier models (cf. Supplementary Information and Supplementary Figure S2).

The positive effects of reducing transporter affinity are only significant under certain conditions. For instance, if the intracellular substrate concentration is very low, substrate efflux is also low and thus hardly a problem. The intracellular substrate concentration depends on the kinetics of its uptake and consumption in metabolism in complex, non-intuitive ways. We therefore used a detailed kinetic model of *S. cerevisiae* glycolysis ([16]adapted from[17]) to test if under realistic conditions reducing the affinity significantly increases the net uptake rate. We calculated the steady-state glycolytic flux as a function of the K_M of the glucose transporter, $K_{M,GLT}$ (Fig. 2B). Indeed, at a high extracellular glucose concentration of 110 mM the low affinity HXT3 carrier ($K_{M,GLT} \approx 34$ mM) attains a 36% higher glycolytic flux than the high affinity HXT6 carrier ($K_{M,GLT} \approx 1.5$ mM). On the other hand, at low extracellular glucose concentration of 5 mM, the HXT6 transporter is expected to be (nearly) optimal. Note that we did not change the transporters V_{max}, such that these difference arise purely from the difference in affinity.

Experimental observations do not discard any of the two hypotheses. Both the trade-off and the reduced efflux hypothesis can be tested using several single transporter strains with (wild-type or mutated) transporters differing in their K_M. The absence of transporters with a high K_M and a high k_{cat} would support the trade-off hypothesis. Moreover, if this hypothesis is true, we would expect the wild-type transporters to be close to the Pareto front. (If a point lays on the Pareto front, there are no other points that have both a higher k_{cat} and a higher affinity.) A higher steady-state uptake rate at saturating substrate concentrations of cells with transporters with the same k_{cat} but a higher K_M would support the reduced efflux hypothesis.

Several labs have generated single glucose transporter strains in yeast. They expressed transporter constructs under constitutive promoters in a yeast glucose-transporter null-mutant. Elbing *et al*. generated chimera of the low-affinity HXT1 and the high-affinity HXT7 *S. cerevisiae* glucose carriers[10]. Kasahara *et al*. studied HXT7[18,19] and the low affinity HXT2[20–23] glucose carrier by either mutating specific residues or by constructing chimeras where specific trans-membrane segments from other carriers were used. For all these strains, the K_M and V_{max} have been measured. However, k_{cat} data are not available. Figure 3 shows the K_M and V_{max} measurements that we collected. The transporters from both labs show decreasing V_{max} with increasing affinity, and there are no constructs with both a low K_M and a high V_{max}. In other words, there appears to be a $V_{max} - 1/K_M$ Pareto-front (dashed gray line). Moreover, the wild-type transporters appear to sit on this Pareto front. Provided the expression levels of the carriers are similar, the V_{max} is a good reflection of the k_{cat}, and these data support a rate-affinity trade-off. However, as we will discuss below, this assumption may not be valid.

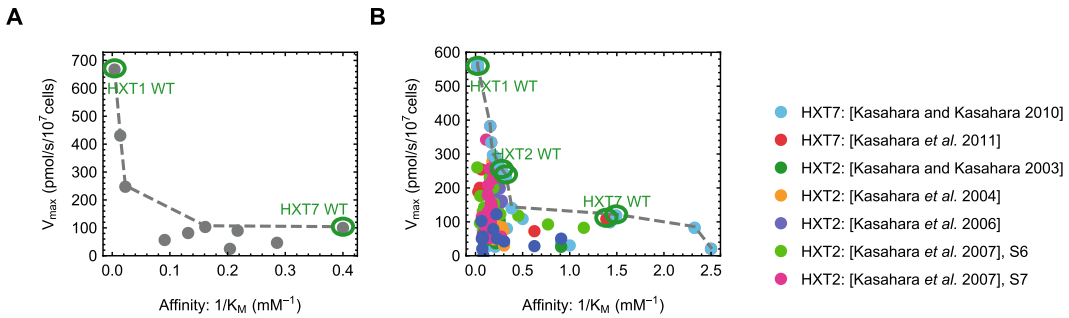

Figure 3. Experimental data suggest a rate-affinity trade-off. Both panels show experimentally established affinities and rates of HXT mutants. (**A**) HXT1-HXT7 chimeras. Data taken from Elbing *et al.*[10] (Converted from per mg of protein to per 10^7 cells using 5 pg protein/cell, BioNumber ID:110550) (**B**) Different HXT2 and HXT7 mutants and chimeras constructed and characterised in the Kasahara lab. References are in the figure legend. The data suggest the existence of a $k_{cat} - 1/K_M$ Pareto-front (gray dashed line), provided the expression levels of all constructs is comparable. The wild-type transporters are located on this front.

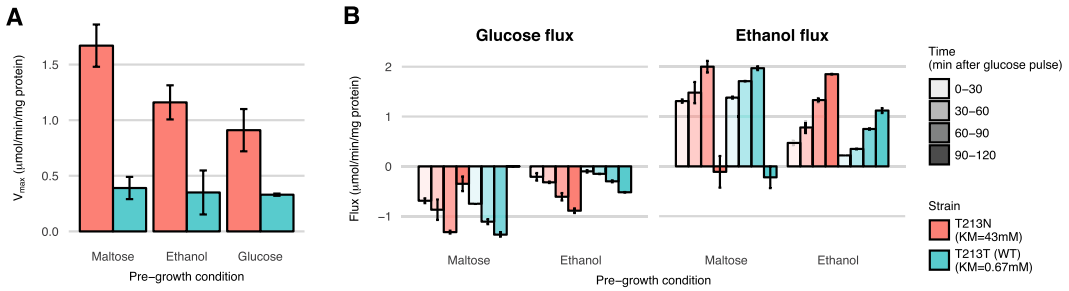

Figure 4. Maximal uptake rate (V_{max}) values and steady-state fluxes for different pre-growth conditions. (**A**) V_{max} values were measured in a 5 s zero-trans uptake assay with 200 mM glucose as substrate. Pre-growth was done on 2% of the carbon source indicated. Prior to the experiment cells were washed in medium without carbon source and incubated for 3′ at 30 °C without a carbon source. Experiments were done in triplicate and shown are the averages with standard deviation. (**B**) Glucose and ethanol concentrations were measured during two hours at 30 °C following a glucose pulse. Protein concentration remained constant throughout the experiment. From this data, specific exchange fluxes were calculated. Shown is the average and standard deviation of two incubations per pre-growth condition.

Strain	*KM* (mM)		V_{max}	
	Kasahara *et al.*[19]	Our strains	Kasahara *et al.*[19] pmol (5 s)$^{-1}$(10^7 cells)$^{-1}$ (ratio vs WT)	Our strains μ mol min^{-1}(mg protein)$^{-1}$ (ratio vs WT)
Low affinity T213N	34 ± 4	43 ± 11	960 ± 50 (1.7)	1.67 ± 0.19 (4.3)
High affinity T213T (WT)	0.72 ± 0.07	0.67 ± 0.05	560 ± 30 (1)	0.39 ± 0.08 (1)

Table 1. Michealis-Menten constants (K_M) and maximal uptake rate (V_{max}) values for glucose transport after pre-growth on maltose.

To test our reduced-efflux hypothesis, we selected two HXT7 constructs from the Kasahara lab that had a similar V_{max} but strongly differed in their K_M: T213N (low affinity; $K_M = 34$ mM) and T213T (the wildtype HXT7 transporter with a high affinity; $K_M = 0.72$ mM)[19]. However, where those authors used transient expression, we integrated the gene into the genome behind the TDH3 promoter to obtain similar expression levels.

To evaluate our strains functionally we determined V_{max} and K_M values of the transporter with a 5 s zero-trans influx uptake assay using radiolabelled glucose[24]. We confirmed the expected K_M-values (see Table 1), but there was a 4-fold difference in V_{max} values between the two strains (Fig. 4A), considerably bigger than the 1.7-fold difference reported in Kasahara[19].

We tested whether there was an effect of the pre-growth conditions. Similar to Kasahara, the measurements above were obtained after pre-growth on maltose. Although we had carbon-starved the cells prior to the uptake assay, it could be that residual internal glucose from the conversion of maltose to glucose during pre-growth inhibits glucose uptake in our experiments. Along the lines of our hypothesis, this would affect the high-affinity strain more than the low-affinity strain and could result in a lower apparent V_{max} in the high-affinity strain. To overcome this potential problem, we grew the cells on the non-glycolytic substrate ethanol and again measured

the V_{max} of glucose transport. Again, the low-affinity strain had a 4-fold higher V_{max} than the high-affinity strain (Fig. 4A). Pre-growth on glucose gave a lower V_{max} for the low-affinity strain, but still there was a 3-fold difference between the low-affinity and the high-affinity strain (Fig. 4A).

Steady-state flux experiments after a glucose pulse revealed further dynamics of uptake and glycolytic flux (Fig. 4B). In the 2 hours after a glucose pulse, the glycolytic flux increases in each 30-minute interval. For cells that were pre-grown on maltose, the steady-state flux in the first 30 minutes exceeded the V_{max} we measured in the first 5 s after the cells were exposed to glucose. This suggests that within 30 minutes the transport capacity was increased. Apparently, despite the genome integration, protein expression of these transporters depends on pre-growth medium, is highly dynamic, and might well differ between the different strains. Therefore, the V_{max} is not a good estimate of the k_{cat}, which makes it hard to test the reduced efflux hypothesis and leaves some uncertainties to the experimental support for the trade-off hypothesis.

Conclusion and Discussion

In this study we examined an existing hypothesis regarding the benefit of using low-affinity transporters, and proposed a new one. It has been postulated that a trade-off between rate and affinity exists, but so far theoretical as well as experimental evidence for this idea was lacking. We showed that for a facilitated diffusion uptake model there are theoretical arguments and experimental results in favour of this notion. However, there is no conclusive proof for this trade-off. We have also provided a novel explanation for the existence of low-affinity carriers, namely that they can reduce substrate efflux and thus enhance the net uptake rate.

The two hypotheses discussed here are not mutually exclusive. A decreased affinity might well be beneficial because it both raises the catalytic efficiency and reduces the substrate efflux. In fact, for the case of glucose uptake in yeast, a combination of a trade-off and the reduction of substrate efflux is probably the more complete explanation. The reduced efflux in that case might be the dominant effect for the high to intermediate affinity modulation. However, since for K_Ms above roughly 30 mM substrate efflux is likely negligible in any case, even lower affinities might be explained by the trade-off.

To test the reduced efflux hypothesis, we integrated the HXT7 isoforms made by Kasahara *et al.*[19] into the genome of a yeast strain lacking glucose transporters. However, while we only expected the HXT7 isoforms to differ in K_M, also their V_{max}-values were different. This difference in V_{max}-values was unexpected. Apparently, despite identical sequence except for one mutation, identical nutrient conditions during pre-growth, and expression from the same promoter (tdh3), there is differential dynamics of the amount of transporters in the membrane in these two strains. Indeed, glucose-induced expression of the tdh-genes has been observed before[25,26], and HXT7 is known to be degraded quickly in response to a glucose pulse[27]. Transporter dynamics could even be affinity-dependent (e.g. through the intracellular glucose levels). As $V_{max} = k_{cat} * [enzyme]$, a difference in V_{max} could still mean the k_{cat}-values are the same in case only the expression of the transporters differs. However, even if the k_{cat}s would be the same, without the same V_{max}-values our hypothesis still cannot be tested. This is because the steady-state intracellular glucose concentration, and as a consequence the magnitude of substrate efflux and the optimal K_M for maximal glycolytic flux depends on the V_{max} of the transporter and not only on the k_{cat}. For instance, a lower V_{max} will reduce the intracellular glucose concentration, which subsequently reduces the substrate efflux and will lower the K_M-value that gives the maximal glycolytic flux (see Supplementary Figure S3). This means that testing our hypothesis requires both the k_{cat} and the V_{max} of two transporters to be similar.

While there are observations that are in line with both hypotheses, the need for a solid experimental tests remains. The trade-off hypothesis could be verified experimentally by systematically measuring k_{cat} and K_M values of a large collection of similar transporters. (Collecting the required set of transporter mutants, do the enzyme kinetics and perform the quantitative membrane proteomics is outside the scope of this study). Those measurements would also allow for the selection of transporters for a renewed attempt to directly test the reduced efflux hypothesis. To tightly control transporter expression levels and other factors that influence the uptake capacity, proteoliposomes with reconstituted transporters could provide an alternative test system[28,29].

Although direct experimental evidence turned out to be compromised by unresolved dynamics in glucose transporter activities, several observations support the reduced efflux hypothesis. First, in cells with high affinity transporters the steady-state glucose uptake rate at saturating extracellular glucose concentrations was up to 50% below the V_{max}, and the measured intracellular glucose concentration was comparable to the transporter's K_M[14]. For low affinity transporters, the steady-state flux matched the V_{max} and the intracellular glucose concentration was well below the K_M[14]. This indicates that intracellular glucose strongly inhibits uptake of the high but not of the low affinity transporter. Second, significant HXT-mediated glucose efflux has been observed in *S. cerevisiae* grown on maltose (maltose is intracellularly metabolized into two glucose molecules)[30]. Third, the affinity, but not the maximal uptake capacity, of glucose transport is modulated during growth on glucose[24].

Our reduced efflux hypothesis could also explain other phenomena besides low affinity uptake systems. For instance, the high affinity MCT1 and low affinity MCT4 lactate transporters in human tissue act as both importers and exporters, depending on the conditions[6]. MCT1 is typically expressed in cell types that import lactate as a substrate for oxidative phosphorylation, such as heart cells and red skeletal muscle, whereas MCT4 is predominantly expressed in cells that export excess lactate as a waste product of glycolysis, such as white skeletal muscle cells during heavy exercise[5]. Since the intracellular lactate concentration during heavy exercise is high, the low affinity MCF4 transporter may be favored because it wouldn't be inhibited by low extracellular lactate.

To conclude, the idea that a lower affinity can result in a higher flux even at constant k_{cat} is perhaps counter-intuitive, but is a direct consequence of the nature of transport processes, i.e. the absence of direct competition between extracellular and intracellular substrates. This enhanced product sensitivity is easily overlooked, and we expect it to be an important driver in systems where nutrient uptake is a relevant component of fitness.

Materials and Methods

Strains and media. The *S. cerevisiae* strains used in this study are listed in Supplementary Table S1.Under non-selective conditions, yeast was grown in complex medium (YPD) containing 10 g/L yeast extract, 20 g/L peptone and 20 g/L glucose. Selective media consisted of synthetic media (SM) containing 3 g/L KH_2PO_4, 0.5 g/L $MgSO_4 \cdot 7H_2O$, 5 g/L $(NH_4)2SO_4$, 1 mL/L of a trace element solution and 1 mL/L of a vitamin solution[31]. Either maltose (SMM) or glucose (SMG) was used as sole carbon source (20 g/L). When necessary, the medium was supplemented to fulfill the auxotrophic requirements of the yeast strains, as previously described[32]. For the uptake experiments, strains were grown at 30 °C using defined mineral medium (CBS)[31] supplemented with required amino acids and 2% maltose or 2% ethanol as indicated.

Strains and plasmids construction. EBY.VW4000, devoid of hexose transporters, was the platform strain for the constitutive expression of the HXT7 isoforms. Repair of the three auxotrophies of this strain (for tryptophan, leucine and histidine), construction of integrative vectors for the HXT7 isoforms and finally integration in EBY.VW4000 genome were the genetic modifications required.

Repair of auxotrophies. The three auxotrophies were repaired in a single transformation event (Supplementary Figure S4).The TRP1 and HIS3 genes were PCR-amplified from the genomic DNA of *S. cerevisiae* CEN.PK113-7D using primers 5890_TRP1 fw, 5891_TRP1 rv, 2335_HIS3 fw and 2336_HIS3 rv, while the LEU2 gene was amplified from the pRS405 plasmid using primers 5892_LEU2 fw and 7052_LEU2 rv (Supplementary Table S2).The primers used for these amplifications were designed to flank the integration cassettes with sequences homologous to the adjacent cassettes (SHR[33]), or to the integration site in order to facilitate simultaneous assembly and integration in the CAN1 locus of EBY.VW4000 via homologous recombination. After transformation of the three integration cassettes to EBY.VW4000, transformants were grown on plates with SMM supplemented with uracil and subsequently replica-plated on SMM supplemented with uracil and L-canavanine (15 mg/L[34]). A single colony was isolated and named IMX746. Proper assembly of the genes in IMX746 was confirmed by diagnostic PCR using the primers 5894_diag CAN1 fw, 5895_diag TRP1 rv, 5896_diag TRP1 fw, 5897_diag HIS3 rv, 5898_diag HIS3 fw, 5899_diag LEU2 rv, 5900_diag LEU2 fw and 5901_diag CAN1 rv (Supplementary Table S2).

Construction of integrative vectors for the HXT7 isoforms. To ensure strong and constitutive expression, the HXT7 isoforms were cloned behind the *S. cerevisiae* TDH3 promoter. To this end, the HXT7 expressing plasmids were constructed by *in vitro* assembly (Gibson assembly) of three parts: a plasmid backbone obtained by PCR amplification of pRS406 using primers 6290_pRS406 fw and 6291_pRS406 rv, the TDH3 promoter PCR-amplified from the genomic DNA of CEN.PK113-7D with primers 6292_TDH2p fw and 6293_TDH3p rv and one of the two HXT7 isoforms amplified from the original Hxt7mnx-pVT T213N and Hxt7mnx-pVT_T213T plasmids constructed by the Kasahara lab[19] using primers 6294_HXT7 fw and 6295_HXT7 rv. All primers are listed in Supplementary Table S3.The PCR products were purified and, when the template for the reaction was a vector, digested with DpnI prior to assembly. Assembly of these parts yielded the integrative plasmids pUDI091 and pUDI093 (Supplementary Table S3).Confirmation of the assembly was done by diagnostic PCR (with primers 6034_diag TDH3p fw, 1852_diag HXT7 rv, 1693_diag URA3 fw, 2613_diag TDH3p rv, 3795_diag ADH1t fw and 3228_diag pRS406 rv; all listed in Supplementary Table S3) and by restriction analysis with BstBI.

Genomic integration of HXT7 isoforms. The strain IMX746 is auxotrophic for uracil due to a large insertion in the URA locus[35]. The cassettes pUDI091 and pUDI093, which carry the URA3 gene next to the HXT7 isoforms, were digested with the restriction enzyme StuI, that has a unique recognition site in the URA3 gene. Each of the linearized vectors were then transformed to the strain IMX746. The linearized vector was integrated at the URA3 locus via single crossover, resulting in the integration of a full copy of the URA3 gene and of the HXT7 isoform. Transformants were grown on plates containing SMG. Single colonies were isolated and named IMI335, for the strain containing the HXT7 T213N isoform and IMI337 for the strain containing the HXT T213T isoform. The sequences of the two HXT7 isoforms were confirmed by Sanger sequencing (Baseclear BV).

Molecular biology techniques. PCR amplification with Phusion Hot Start II high-fidelity polymerase (Thermo Scientific, Waltham, MA) was performed according to manufacturer's instruction using HPLC purified custom-synthesized oligonucleotide primers (Sigma-Aldrich). Diagnostic PCR was done with DreamTaq (Thermo Scientific) and desalted primers (Sigma-Aldrich). DNA fragments obtained by PCR were loaded on gel containing 1% (wt/vol) agarose (Thermo Scientific) and 1x Tris-acetate EDTA buffer (Thermo Scientific) and, when necessary, purified using the Zymoclean kit (Zymo Research, Irvine, CA). Propagation of plasmids was performed in chemically competent *E. coli* DH5 α according to manufacturer instructions (Z-competent transformation kit, Zymo Research). Restriction analysis were performed with FastDigest enzymes DpnI, StuI and conventional enzyme BstBI (Thermo Scientific). Plasmids were isolated from *E. coli* with GenElute Plasmid kit (Sigma-Aldrich). Genomic DNA from yeast was extracted with YeaStar genomic DNA kit (Zymo Research). Cultures for transformation were grown overnight in complex medium with maltose. DNA concentrations of the cassettes for transformation were measured in a NanoDrop 2000 spectrophotometer (wavelength 260 nm, Thermo Fisher Scientific) and when necessary, pooled prior to transformation maintaining equimolar concentrations. Transformation to yeast was performed with the LiAc/ssDNA method described by Gietz *et al.*[36].

Uptake experiments. *Mid-exponential phase cells for steady-state flux experiments.* Cells of two glycerol stocks of 1 ml were washed with 10 ml CBS medium (depending on the experiment with 2% maltose or 2% ethanol). The cells were cultured overnight in 10 ml medium CBS with 2% maltose or 2% ethanol on a shaker at 30 °C and 200 rpm. The culture was diluted to OD 0.2 in two separate 250 ml Erlenmeyer flasks, each with 50 ml CBS with

2% maltose or 2% ethanol. Cultures were kept separate as duplicates. Cells were grown at 30 °C and 200 rpm until OD 4 and then diluted to OD 0.35 in 500 ml CBS with 2% maltose or 2% ethanol in 1 L erlenmeyer flasks. Cells were harvested at OD 4. Cells were pelleted at 1700 g for 15 minutes and washed with 500 ml CBS without carbon source. The pellet was re-suspended in CBS medium without carbon source to OD 40. The volume was measured and the cells were poured in a 100 ml beaker for the experiment.

Steady-state flux measurements. The assay was performed at 30 °C. The cell suspension was stirred continuously. Samples for protein determination and metabolite concentration were taken prior to the start of the experiment. At time zero glucose was added to a final concentration of 4%. Samples were taken every 5 minutes during the first hour after addition of glucose and every 30 minutes during the second hour. For the glucose and ethanol concentration determination 0.1 ml sample was added to 0.9 ml 70% perchloric acid (PCA) and stored at −80 °C. After thawing, the pH of the samples was adjusted to 4–5 with 185 μL 7 M KOH. Samples were centrifuged and the supernatant was filtered through 0.22 μm syringe filter. The glucose and ethanol concentrations were determined with a Shimadzu LC20-AT HPLC and a Rezex (Phenomenex) column at 55 °C. The flow of the eluent (5 mM H_2SO_4) was 0.5 ml/min. Glucose and ethanol fluxes were calculated in μmol/min/mg-protein.

Mid-exponential phase cells for zero trans influx uptake experiments. Cells of a glycerol stock of 1 ml were washed with 10 ml medium CBS (depending on the experiment with 2% maltose, 2% ethanol or 2% glucose). The cells were cultured overnight in 10 ml medium CBS with 2% maltose, 2% ethanol or 2% glucose on a shaker at 30 °C and 200 rpm. The culture was added to 50 ml medium CBS with 2% maltose, 2% ethanol or 2% glucose in a 250 ml Erlenmeyer flasks and grown until ~OD 0.7, then the culture was diluted to ~OD 0.1 in three 250 ml Erlenmeyer flasks, each with 50 ml CBS with 2% maltose, 2% ethanol or 2% glucose. Cultures were kept separate as triplicates. Cells were grown at 30 °C and 200 rpm until ~OD 3. Cells were pelleted at 1700 g for 15 minutes and washed with 50 ml CBS without carbon source. The pellet was re-suspended in CBS medium without carbon source to ~OD 80 and stored on ice. Prior to the uptake assay cells were put at 30 °C with aeration for 3 minutes to deplete intracellular glucose.

Zero trans influx glucose uptake assay. The zero-trans influx of ^{14}C-labeled glucose was determined in a 5 s assay, described by Walsh *et al.*[24] with the modifications of Rossell *et al.*[37]. The range of glucose concentrations used was between 0.25 and 200 mM. Irreversible Michaelis-Menten equations were fitted to the data by non-linear regression.

Protein samples and protein assay. For the steady-state flux experiments 0.25 ml sample was added to 0.75 ml CBS medium without carbon source and kept on ice. Cells were centrifuged for 2 minutes at maximal speed in a table centrifuge at 4 °C, washed with 1 ml ice cold water, pelleted and resuspended in 1 ml ice-cold 0.1 M NaOH. For the zero-trans-influx uptake experiments, 0.1 ml of the cell suspension was added to a mix of 0.1 ml NaOH 10 M and 0.8 ml demi water for the protein concentration. The samples were stored at −20 °C. After thawing the samples were boiled for 10 minutes at 110 °C, cooled down and centrifuged for 2 minutes at maximum speed. The supernatant was used for the protein determination with the Pierce BCA assay and compared to a dilution curve of BSA.

Model simulations. The simulation of Fig. 2B are made using a kinetic model of *S. cerevisiae* glycolysis[16]. The model is available on JWS online[38] under the model ID vanHeerden1. We obtained the steady state flux for a given K_M of the transporter and extracellular substrate concentration by first running a time simulation for 10000 minutes. We then use the metabolite levels from the time simulation to find a local steady state. We plot the glucose transport rate from this steady state in mM/min/L-cytosol as the glycolysis rate.

Data availability. The yeast glycolysis model is available on JWS online[38] (ID: vanHeerden1) under the following link: https://jjj.bio.vu.nl/models/vanheerden1/. The strains used in this study are available upon request.

References

1. Boles, E. & Hollenberg, C. The molecular genetics of hexose transport in yeasts. *FEMS Microbiol. Rev.* **21**, 85–111 (1997).
2. Thorens, B. & Mueckler, M. Glucose transporters in the 21st Century. *Am. J. Physiol. Endocrinol. Metab.* **298**, E141–5 (2010).
3. Castro, R. *et al*. Characterization of the individual glucose uptake systems of *Lactococcus lactis*: mannose-PTS, cellobiose-PTS and the novel GlcU permease. *Mol. Microbiol.* **71**, 795–806 (2009).
4. Levy, S., Kafri, M., Carmi, M. & Barkai, N. The Competitive Advantage of a Dual-Transporter System. *Science* **334**, 1408–1412 (2011).
5. Bonen, A. *et al*. Abundance and subcellular distribution of MCT1 and MCT4 in heart and fast-twitch skeletal muscles. *Am. J. Physiol. Endocrinol. Metab.* **278**, E1067–77 (2000).
6. Juel, C. & Halestrap, A. Lactate transport in skeletal muscle–role and regulation of the monocarboxylate transporter. *J. Physiol.* **517**, 633–642 (1999).
7. Liu, K.-H. & Tsay, Y.-F. Switching between the two action modes of the dual-affinity nitrate transporter CHL1 by phosphorylation. *EMBO J.* **22**, 1005–13 (2003).
8. Youk, H. & Oudenaarden, A. V. Growth landscape formed by perception and import of glucose in yeast. *Nature* **462**, 875–879 (2009).
9. Gudelj, I., Beardmore, R. E., Arkin, S. & MacLean, R. C. Constraints on microbial metabolism drive evolutionary diversification in homogeneous environments. *J. Evol. Biol.* **20**, 1882–1889 (2007).
10. Elbing, K. *et al*. Role of hexose transport in control of glycolytic flux in *Saccharomyces cerevisiae*. *Appl. Environ. Microbiol.* **70**, 5323–5330 (2004).
11. Szenk, M., Dill, K. A. & de Graff, A. M. Why do fast-growing bacteria enter overflow metabolism? testing the membrane real estate hypothesis. *Cell Systems* **5**, 95–104 (2017).
12. Heinrich, R., Schuster, S. & Holzhütter, H.-G. Mathematical analysis of enzymic reaction systems using optimization principles. *Eur. J. Biochem.* **201**, 1–21 (1991).
13. Klipp, E. & Heinrich, R. Evolutionary optimization of enzyme kinetic parameters; effect of constraints. *J. Theor. Biol.* **171**, 309–23 (1994).
14. Teusink, B., Diderich, J. A., Westerhoff, H. V., van Dam, K. & Walsh, M. C. Intracellular glucose concentration in derepressed yeast cells consuming glucose is high enough to reduce the glucose transport rate by 50%. *J. Bacteriol.* **180**, 556–62 (1998).

15. Maier, A., Voelker, B., Boles, E. & Fuhrmann, G. F. Characterisation of glucose transport in *Saccharomyces cerevisiae* with plasma membrane vesicles (countertransport) and intact cells (initial uptake) with single hxt1, hxt2, hxt3, hxt4, hxt6, hxt7 or gal2 transporters. *FEMS yeast* **2**, 539–550 (2002).
16. van Heerden, J. H. *et al.* Lost in Transition: Startup of Glycolysis Yields Subpopulations of Nongrowing Cells. *Science* **343** (2014).
17. Teusink, B. *et al.* Can yeast glycolysis be understood in terms of *in vitro* kinetics of the constituent enzymes? Testing biochemistry. *Eur. J. Biochem.* **267**, 5313–29 (2000).
18. Kasahara, T. & Kasahara, M. Identification of a key residue determining substrate affinity in the yeast glucose transporter Hxt7: a two-dimensional comprehensive study. *J. Biol. Chem.* **285**, 26263–8 (2010).
19. Kasahara, T., Shimogawara, K. & Kasahara, M. Crucial effects of amino acid side chain length in transmembrane segment 5 on substrate affinity in yeast glucose transporter Hxt7. *Biochemistry* **50**, 8674–81 (2011).
20. Kasahara, T. & Kasahara, M. Transmembrane segments 1, 5, 7 and 8 are required for high-affinity glucose transport by *Saccharomyces cerevisiae* Hxt2 transporter. *Biochem. J.* **372**, 247–52 (2003).
21. Kasahara, T., Ishiguro, M. & Kasahara, M. Comprehensive chimeric analysis of amino acid residues critical for high affinity glucose transport by Hxt2 of *Saccharomyces cerevisiae*. *J. Biol. Chem.* **279**, 30274–8 (2004).
22. Kasahara, T., Ishiguro, M. & Kasahara, M. Eight amino acid residues in transmembrane segments of yeast glucose transporter Hxt2 are required for high affinity transport. *J. Biol. Chem.* **281**, 18532–8 (2006).
23. Kasahara, T., Maeda, M., Ishiguro, M. & Kasahara, M. Identification by comprehensive chimeric analysis of a key residue responsible for high affinity glucose transport by yeast HXT2. *J. Biol. Chem.* **282**, 13146–50 (2007).
24. Walsh, M. C., Smits, H.-P., Scholte, M. & van Dam, K. Affinity of Glucose Transport in *Saccharomyces cerevisiae* Is Modulated during Growth on Glucose. *J. Bacteriol.* **176**, 953–958 (1994).
25. Hommes, F. Effect of glucose on the level of glycolytic enzymes in yeast. *Archives of biochemistry and biophysics* **114**, 231–233 (1966).
26. Maitra, P. & Lobo, Z. A kinetic study of glycolytic enzyme synthesis in yeast. *Journal of Biological Chemistry* **246**, 475–488 (1971).
27. Krampe, S., Stamm, O., Hollenberg, C. P. & Boles, E. Catabolite inactivation of the high-affinity hexose transporters hxt6 and hxt7 of saccharomyces cerevisiae occurs in the vacuole after internalization by endocytosis 1. *FEBS letters* **441**, 343–347 (1998).
28. Hansen, J. S., Elbing, K., Thompson, J. R., Malmstadt, N. & Lindkvist-Petersson, K. Glucose transport machinery reconstituted in cell models. *Chem Commun (Camb)* **51**, 2316–9 (2015).
29. Madej, M. G., Sun, L., Yan, N. & Kaback, H. R. Functional architecture of mfs d-glucose transporters. *Proceedings of the National Academy of Sciences* **111**, E719–E727 (2014).
30. Jansen, M. L. A., De Winde, J. H. & Pronk, J. T. Hxt-Carrier-Mediated Glucose Efflux upon Exposure of *Saccharomyces cerevisiae* to Excess Maltose. *Appl. Environ. Microbiol.* **68**, 4259–4265 (2002).
31. Verduyn, C., Postma, E., Scheffers, W. A. & Van Dijken, J. P. Effect of benzoic acid on metabolic fluxes in yeasts: a continuous-culture study on the regulation of respiration and alcoholic fermentation. *Yeast* **8**, 501–517 (1992).
32. Pronk, J. T. Auxotrophic yeast strains in fundamental and applied research. *Applied and environmental microbiology* **68**, 2095–2100 (2002).
33. Kuijpers, N. G. *et al.* A versatile, efficient strategy for assembly of multi-fragment expression vectors in saccharomyces cerevisiae using 60 bp synthetic recombination sequences. *Microbial cell factories* **12**, 47 (2013).
34. Solis-Escalante, D. *et al.* amdsym, a new dominant recyclable marker cassette for saccharomyces cerevisiae. *FEMS yeast research* **13**, 126–139 (2013).
35. Rose, M. & Winston, F. Identification of a ty insertion within the coding sequence of the s. cerevisiae ura3 gene. *Molecular and General Genetics MGG* **193**, 557–560 (1984).
36. Gietz, R. D. & Woods, R. A. Transformation of yeast by lithium acetate/single-stranded carrier dna/polyethylene glycol method. *Methods in enzymology* **350**, 87–96 (2002).
37. Rossell, S., van der Weijden, C. C., Kruckeberg, A. L., Bakker, B. M. & Westerhoff, H. V. Hierarchical and metabolic regulation of glucose influx in starved saccharomyces cerevisiae. *FEMS yeast research* **5**, 611–619 (2005).
38. Olivier, B. G. & Snoep, J. L. Web-based kinetic modelling using jws online. *Bioinformatics* **20**, 2143–2144 (2004).

Acknowledgements

This work was supported by NWO-VICI grant 865.14.005, and by projects funded by the Netherlands Genomics Initiative. We thank prof. Kasahara for kindly providing the HXT7 constructs, prof. Pascale Daran-Lapujade for help with integrating these into the genome, and Jose Gavaldá García for help with performing pilot experiments. Some elements of Fig. 1 are reused from a figure uploaded to Wikimedia Commons by Mariana Ruiz Villarreal.

Author Contributions

E.B., M.T.W. and B.T. designed the research. E.B. and M.T.W. developed the mathematical models and performed numerical simulations and theoretical analysis. P.T.C. integrated the constructs into the genome. J.R.H. and M.J.W. performed the experiments. E.B., M.T.W. and J.R.H. wrote the manuscript. All authors read and approved the manuscript.

Additional Information

Supplementary information accompanies this paper at https://doi.org/10.1038/s41598-018-23528-7.

Competing Interests: The authors declare no competing interests.

Publisher's note: Springer Nature remains neutral with regard to jurisdictional claims in published maps and institutional affiliations.